# Optical absorption and localization of eigenmodes in disordered clusters

Mark I. Stockman,* Lakshmi N. Pandey, Leonid S. Muratov,*,† and Thomas F. George
*Departments of Physics and Chemistry, Washington State University, Pullman, Washington 99164-2814*
(Received 18 July 1994)

Results of a large-scale computational project for the calculation of the dispersion relations of eigenmodes (surface plasmons) and optical-absorption spectra of disordered clusters (fractal and uncorrelated) are reported. Fractals (cluster-cluster aggregates and the random-walk clusters, both original and diluted) and random-gas clusters consisting of 100–300 monomers are studied. High-accuracy results of Monte Carlo simulations are obtained. Transition of the eigenmodes from extremely localized to fully delocalized is found. Scaling of the dispersion relation of the eigenmodes, i.e., their localization radius or coherence length as a function of the spectral variable $X$, predicted earlier is quantitatively confirmed for diluted clusters. In contrast to the dispersion relations, the absorption spectra as functions of $X$ do not show pronounced scaling in the intermediate region, but scale in the binary (spectral-wing) region. We suggest a new plot for the absorption profiles, namely absorption as a function of the coherence length of excitations. In such plots for most clusters, scaling is pronounced, but the indices differ dramatically from the predictions of the strong-localization theory. Possible reasons for the observed behavior are discussed.

## I. INTRODUCTION

There has been recently an increased interest in the optics of fractal clusters (we will call them simply "fractals" below) and composites; see, e.g., Refs. 1–23. This interest is mostly associated with enhanced nonlinear optical responses of fractals predicted[4] and studied both theoretically[14,20] and experimentally.[5,6,8,12,15,19] Fractals are self-similar clusters built of some constituent particles which are called monomers and whose properties are considered as known. Unusual optical properties of fractals are associated with their self-similarity. One of the implications of the self-similarity is a very low, asymptotically-zero, mean density of fractals, $\bar{\rho}\sim(R_c/R_0)^{D-3}$, where $D$ is the Hausdorff dimension of a fractal, $R_c$ is its total size, and $R_0$ is a characteristic (average) distance between its nearest-neighbor monomers. In fact, $\bar{\rho}\to 0$ for $R_c/R_0\to\infty$ for any nontrivial fractal ($D<3$). Not only the mean three-dimensional density of fractals vanishes, but also a two-dimensional density (i.e., the density of a fractal projected to a plane) vanishes for $D<2$ as $(R_c/R_0)^{D-2}$. This fact is closely related to the result of Ref. 1 that light-scattering probability from a fractal with $D<2$ is proportional to the number $N$ of monomers in a fractal, $N\sim(R_c/R_0)^D$. Physically, this implies that a fractal with $D<2$ is asymptotically (i.e., for $R_c\gg R_0$) transparent to light.

Asymptotically-zero density precludes use of mean-field approaches to describe optical properties of fractals. In particular, the Lorentz local field diverges at small distances $r$ as $r^{D-3}$ (Refs. 3 and 4). Due to the impossibility of using mean-field theories even as a zeroth-order approximation, the theory of linear responses of fractals poses a formidable problem. There have been developed some approaches to deal with this problem in finding linear optical responses.

A differential effective medium theory has been used to average over different scales in a fractal.[2] A spectral approach has been suggested[7] and employed in both analytical theory and numerical calculations. Scaling dependences of the absorption and the coherence length of excitations (surface plasmons)[24] on a specially chosen spectral variable $X$ (see below) for random fractal clusters with the dipole interaction between monomers have been predicted.[7] This scaling is governed by an index $d_0$ called the optical spectral dimension.

Another form of the spectral approach has been developed[10] for exactly self-similar recursively built fractals with the dipole interaction. An approximate renormalization scheme in Ref. 10 has allowed one to obtain numerically the spectra of such fractals. Due to nonrandomness and exact self-similarity of fractals in Ref. 10, the spectrum of eigenmodes is shown to be a multifractal set[25] with no well-defined smooth envelope.

Strong localization of the dipole eigenmodes (surface plasmons) of fractals has been predicted.[7,9] A qualitative numerical confirmation of such localization has subsequently been obtained.[18] Very recently, experimental evidence has been obtained which directly supports the localization.[22]

A generalization of the effective-medium theory of Ref. 2 dealing with conductivities of deterministic fractal lattices has been developed.[23] This theory supports the idea of Refs. 7 and 9 on the crossover from localized to delocalized surface plasmons and gives a wide range of scaling predictions. However, the interaction in Ref. 23 is only between the nearest neighbors, while in our theory[7,9] each monomer interacts with all other monomers.

The properties of linear spectra are closely related to the presence of very strong fluctuations of local fields in fractals.[3,7,9,21] These fluctuations ultimately limit usefulness of mean-field approximation for fractals. In fact, the

 

dispersion of local-field intensity is on the order of its squared mean, so that the mean local field is to no extent a sufficient characteristic. On the other hand, the local-field fluctuations in fractals bring about strong enhancement of nonlinear responses[4,14] and surface-enhanced Raman scattering.[16] In this respect, the situation in fractals differs from that in nonfractal composites where a significant enhancement can be achieved due to high *average* local fields.[26]

Because the linear responses are reflective of the local fields, and the latter constitutes the basis for a wealth of enhanced optical phenomena, accurate information on the linear polarizabilities of fractals and the underlying eigenmodes is of prime importance for the theory. The previous Monte Carlo calculations of Refs. 7, 9, 17, and 18 do not have the necessary accuracy due to insufficient statistics and small size of individual clusters. Actually, there is not available any serious quantitative comparison of the analytically obtained predictions of Refs. 7 and 9 with a numerical experiment based on high-resolution computations.

In this paper we report the results of large-scale high-precision Monte Carlo calculations. We have accurately determined the linear spectra and eigenmode distribution and have calculated the dispersion relations of the eigenmodes. The different predictions of the scaling theory are compared with the results of the numerical experiment, and some of the results of such a comparison are quite unexpected. We conclude that there is no considerable scaling behavior in the spectral variable $X$ for the linear polarizability and the eigenmode density, but some of the calculated dispersion relations are consistent with the scaling. We suggest a new plot, optical absorption vs coherence length, having the advantage of *both* the function and argument being potentially scale invariant. The plots calculated do reveal a pronounced scaling behavior in most cases, but the corresponding indices are different from those analytically predicted.

In Sec. II we very briefly recapitulate the basic equations and discuss the scaling properties of the linear polarizability. In Sec. III we present results for the dispersion relation and the localization of the fractal eigenmodes. In Sec. IV we consider the linear spectra and the eigenmode distribution. In Sec. V we briefly discuss the obtained results.

## II. BASIC EQUATIONS

To make the paper as self-contained as possible, we will very briefly summarize below some results of the theory of Refs. 7 and 9. In passing, we will introduce necessary definitions and notations.

We consider a fractal cluster of $N$ monomers positioned at points $\mathbf{r}_i (i=1,\ldots,N)$ subjected to an external electric field $\mathbf{E}^{(0)}$ oscillating at the optical frequency. We assume that the total size of the cluster $R_c$ is much less than the light wavelength $\lambda$. Thus the field $\mathbf{E}^{(0)}$ is the same at each monomer. This field polarizes monomers inducing oscillating dipole moments $\mathbf{d}_i$ which are random quantities due to the random structure of the fractal. Instead of $3N$ quantities $d_{i\alpha}$ $(i=1,\ldots,N,\ \alpha=x,y,z)$, we introduce a single $3N$-dimensional vector $|d)$ with components $(i\alpha|d)=d_{i\alpha}$. Similar notations will be used for other local vector quantities.

We assume that the interaction between monomers at the optical frequency is dipolar and a monomer has an isotropic dipole polarizability $\alpha_0$ at the optical frequency.[27] In the above-mentioned notations, the basic equations acquire the form of a vector equation in a $3N$-dimensional space,[7]

$$(Z+W)|d)=|E^{(0)}) , \tag{1}$$

where $Z=\alpha_0^{-1}$ and $W$ is the dipole-interaction operator,

$$(i\alpha|W|j\beta)=\begin{cases}[r_{ij}^2\delta_{\alpha\beta}-3(\mathbf{r}_{ij})_\alpha(\mathbf{r}_{ij})_\beta]r_{ij}^{-5} , & i\neq j , \\ 0, & i=j , \end{cases} \tag{2}$$

with $\mathbf{r}_{ij}=\mathbf{r}_i-\mathbf{r}_j$, and the Greek letters in subscripts denote vector indices.

The Green function of Eq. (1) is expressed as

$$\mathcal{G}_{i\alpha j\beta}=\left(i\alpha\left|\frac{1}{Z+W}\right|j\beta\right) . \tag{3}$$

Introducing the eigenvectors $|m)$ and corresponding eigenvalues $w_m$ of the $W$ operator in the form of Ref. 13, we find the spectral representation of $\mathcal{G}$ as

$$\mathcal{G}_{i\alpha j\beta}(Z)=\sum_m (i\alpha|m)(j\beta|M)\frac{1}{w_m-X-i\delta} , \tag{4}$$

where $X=-\mathrm{Re}Z$, $\delta=-\mathrm{Im}Z$. The spectral variable $X$ determines the detuning from the surface plasmon resonance in an isolated monomer (such a resonance is determined by the equation $\mathrm{Re}\alpha_0=0$ and, consequently, $X=0$),[24] and $\delta$ describes dielectric losses. We note that a similar spectral approach applied to the optical properties of clusters was independently developed by Fuchs and Claro (Refs. 10 and 28). The spectral variable $y$ of Ref. 10 is directly proportional to our $X$.

The polarizability of a cluster per monomer $\alpha$ averaged over the cluster orientation and density $\nu$ of its eigenmodes smoothed over the interval of $\delta$ are expressed in terms of $\mathcal{G}$ as

$$\alpha(Z)=\frac{1}{3N}\sum_{i,j,\alpha}\langle\mathcal{G}_{i\alpha j\alpha}(Z)\rangle = \frac{1}{3N}\sum_{n,i,j,\alpha}\left\langle\frac{(n|i\alpha)(n|j\alpha)}{w_n-X-i\delta}\right\rangle , \tag{5}$$

$$\nu(Z)=\frac{1}{\pi N}\sum_{i,\alpha}\mathrm{Im}\langle\mathcal{G}_{i\alpha i\alpha}(Z)\rangle = \frac{1}{\pi N}\sum_n\left\langle\frac{\delta}{(X-w_n)^2+\delta^2}\right\rangle , \tag{6}$$

where $\langle\cdots\rangle$ denotes the mean over the ensemble of clusters. The formulas of Eqs. (4)–(6) constitute a basis both for analytical theory and numerical computations (see below and in Sec. III).

Now let us summarize the scaling arguments. We assume that there exists a range of eigenvalues $w_n$ (called below the localization region) for which the polar eigen-

modes (surface plasmons) are well localized within a cluster. This means that the localization radius $L_n$ of such modes should be much less than the cluster size, $L_n \ll R_c$. This assumption is subject to verification, and it proves to be consistent with the final results (see Sec. III).

We assume that the dissipation is low enough, $\delta \ll w_n$, for the relevant eigenmodes (see below in this paragraph). Then we conventionally obtain from Eq. (4)

$$\mathrm{Im}\mathcal{G}_{i\alpha j\beta}=\pi\sum_m (i\alpha|m)(j\beta|m)\delta(w_m-X) , \tag{7}$$

$$\mathrm{Re}\mathcal{G}_{i\alpha j\beta}=\sum_m (i\alpha|m)(j\beta|m)\mathcal{P}\frac{1}{w_m-X} , \tag{8}$$

where $\mathcal{P}$ denotes principal value. It follows from Eqs. (7) and (8) that the external "frequency" $X$ selects the eigenmodes with $w_n \approx X$ for $\mathrm{Im}\mathcal{G}$ due to the presence of the $\delta$ function. However, such a selection is absent for $\mathrm{Re}\mathcal{G}$ where both the low-frequency eigenmodes delocalized over the whole cluster ($L_X \sim R_c$) and the high-frequency eigenmodes localized on just a few monomers ($L_X \sim R_0$) contribute for any $X$ This is the underlying reason for our expectation that $\mathrm{Im}\mathcal{G}$, $\mathrm{Im}\alpha$, and $\nu$, but not $\mathrm{Re}\mathcal{G}$ and $\mathrm{Re}\alpha$, may scale in $X$.

Assuming that $L_X \ll R_c$, we conclude that the eigenmodes with $w_n = X$ are well localized inside the cluster and cannot feel its maximum size $R_c$. Therefore, a single spatial dimension the eigenmodes can depend on is the minimum scale $R_0$ (an average separation between the nearest monomers). For $L_X \ll R_c$, the absorption per monomer, $\alpha$, cannot depend on the number of monomers in the cluster. In this case, as follows from the structures of the dipole interaction (2) and Eq. (7), the dependence of $\mathrm{Im}\alpha$ on $R_0$ and $X$ can only have the form

$$\mathrm{Im}\alpha(X)=R_0^3 F(R_0^3 X) , \tag{9}$$

where $F$ is some function.

Now let us consider $X$ such that the eigenmodes with $w_n = X$ are delocalized over distances much greater than $R_0$ but are still well confined with the cluster size $R_c$, i.e., that

$$R_0 \ll L_X \ll R_c . \tag{10}$$

In this case, the eigenmodes are insensitive also to the minimum scale $R_0$. This suggest that the function $F$ of Eq. (9) is a power function, i.e.,

$$\mathrm{Im}\alpha(X) \propto R_0^3 (R_0^3|X|)^{d_0-1} , \tag{11}$$

where $d_0$ is an index called the optical spectral dimension. As shown in Ref. 7, $\nu(X)$ scales with the same index.

Now we assume that in the region (10) the total absorption of a cluster is scale invariant, i.e., it does not depend on $R_0$. We also assume strong localization of the eigenmodes. This means that $L_X$ is the single length characterizing the eigenmodes with $w_m = X$, which is simultaneously the wavelength and the localization length (i.e., the eigenmodes are actually aperiodic in space). Given that $\alpha$ has the dimensionality of volume and the total absorption is proportional to the number of monomers, a single possible form satisfying these requirements is

$$N\,\mathrm{Im}\alpha(X) \sim L_X^3 (R_c/L_X)^D . \tag{12}$$

Comparing Eq. (12) with Eq. (11), we reproduce the dispersion relation of the eigenmodes (surface plasmons) found in Ref. 7:

$$L_X \sim R_0 (R_0^3|X|)^{-\theta} , \quad \text{where } \theta=\frac{1-d_0}{3-D} . \tag{13}$$

Substitution of Eq. (13) into Eq. (10) yields the scaling condition[7,9] in terms of $X$:

$$N^{-\frac{3/D-1}{1-d_0}} \ll R_0^3|X| \ll 1 , \tag{14}$$

with the additional condition $|X| \gg \delta$.

There is no general prescription to formulate a microscopic expression for $L_X$. One possibility is to define $L_X$ as the rms radius of the excitations,

$$L_X^2=\left\langle \frac{\sum_n \nu_n \left[\sum_{i,\alpha} \mathbf{r}_i^2 (n|i\alpha)^2 - \left[\sum_{i\alpha} \mathbf{r}_i (n|i\alpha)^2\right]^2\right]}{\sum_n \nu_n} \right\rangle , \tag{15}$$

where $\nu_n=[(X-w_n)^2+\delta^2]^{-1}$. This definition is similar to that of Refs. 11 and 18, differing only by the way of averaging [the present one appears to yield a better statistical convergence due to the compensation of the fluctuations in the numerator and denominator of Eq. (15)]. In Eq. (15), $(n|i\alpha)^2$ gives the probability that an $n$th eigenmode is localized on the $i$th monomer with polarization $\alpha$, and the different eigenmodes enter with the same weights $\nu_n(X)$ as in Eq. (6). The Lorentzian form of $\nu_n(X)$ implies a homogeneous spectral contour of the monomers. If the strong-localization assumption is correct, than there exists only one characteristic length, and different ways of finding $L_X$ will yield results which may differ only by constant factors.

We conclude this section with a very brief summary of the binary approximation.[3,7,9] This approximation is valid for $R_0^3|X| \gtrsim 1$ where the corresponding eigenmodes are strongly localized. In this case, the most important interaction of any given monomer is that with its nearest neighbor. In the binary approximation, the polarizability and the eigenmode density are expressed as[9]

$$\alpha(X)=\frac{1}{3}\int_0^\infty [2(Z+r^{-3})^{-1}+(Z-2r^{-3})^{-1}]\rho(r)dr , \tag{16}$$

$$\nu(X)=\frac{1}{2}\int_0^\infty [2\delta(|X|-2r^{-3})]\rho(r)dr , \tag{17}$$

where $\delta(\cdots)$ is the Dirac $\delta$ function (not to be confused with the dissipation parameter $\delta$ which can be formally distinguished by being always used without any argument), and $\rho(r)$ is the nearest-neighbor density. We note

that $\nu(X)$ is an even function of $X$, while $\mathrm{Im}\alpha(X)$ is not. In the far wings of the spectral contour, $R_0^3|X| \gg 1$, for diluted fractals one can use an approximation $\rho(r) \approx Dr^{D-1}$ and obtain asymptotically[9]

$$\mathrm{Im}\alpha(X) \approx \frac{2\pi D}{9} R_0^3 (R_0^3|X|)^{1+D/3} [\Theta(X) + 2^{D/3-1}\Theta(-X)] , \quad (18)$$

$$\nu(X) \approx \frac{D}{3} R_0^3 (R_0^3|X|)^{1+D/3} (1+2^{D/3-1}) , \quad (19)$$

where $\Theta(X)$ is the Heaviside unit-step function. Finally, we note that in this approximation both $\alpha$ and $\nu$ scale as $\alpha(X) \sim \nu(X) \sim R_0^3 (R_0^3|X|)^{1+D/3}$.

## III. NUMERICAL RESULTS: DISPERSION RELATION

We have carried out numerical simulations on the basis of Eqs. (4)–(6) employing Lanczos algorithms[29] to compute eigenvectors and eigenvalues of the $W$ operator [Eq. (2)]. Four types of fractal clusters have been used: random walk (RW), diluted random walk (DRW), cluster-cluster aggregates[30,31] (CCA), and diluted CCA (DCCA). The RW clusters have been obtained using random directions and uniformly distributed length of steps, and the CCA clusters have been generated on a cubic lattice. Numerical calculations include 1000 clusters of each of the four types, with each cluster containing $N=300$ monomers (control calculations with $N=100$ have also been performed).

Diluted clusters have been generated from the original RW and CCA clusters by the decimation algorithm.[7,9] Briefly, each monomer of the original cluster is selected in turn and in random with probability $1-\beta$ is removed from the cluster. The average amount of monomers in the cluster is reduced through such a decimation by a factor of $\beta \ll 1$. The average distance $R_0$ between the nearest monomers left in the cluster is increased by a factor $\beta^{-1/D}$. The degree of dilution in the present computations is $\beta = 10^{-4}$ for RW$\rightarrow$DRW clusters and $\beta = 0.07$ for CCA$\rightarrow$DCCA clusters (obtaining much higher dilution for DCCA would require generation of very large original CCA clusters and, consequently, unrealistically large CPU time on the existing supercomputers). Finally, all clusters are rescaled to obtain $R_0 = 1$. A diluted cluster simulates a collection of monomers obtained by random doping of a fractal network, say, a fractal polymer. The dilution (decimation) does not change the fractal dimensions of the cluster, $D$ (thus, $D=2$ for RW and DRW, and $D \approx 1.7$ for CCA and DCCA), but does simplify its structure at the minimum scale.

We start from the results on the dispersion relation of the eigenmodes (surface plasmons), i.e., the dependence of $L_X$ on $X$ to test the strong-localization and scaling predictions of Ref. 7. The dispersion curves $L_X(X)$ calculated according to Eq. (15) for RW and DRW are given in Fig. 1 and for CCA and DCAA clusters in Fig. 2. In these figures, the values of $L_X$ are normalized to $R_c$ defined as the gyration radius of the clusters, $R_c^2 = N^{-1}\langle \sum_i \mathbf{r}_i^2 \rangle$, and the argument $X$ and the parameter $\delta$ are expressed in terms of $R_0^3|X|$ and $R_0^3\delta$. Due to such a normalization, the resulting curves in Figs. 1 and 2 do not depend on the unit length chosen in the calculations, and they are the same for all geometrically similar clusters. There has been observed a weak dependence on $\delta$ which plays here the role of an interval of averaging. The true dispersion curves are those for $R_0^3\delta \leq 0.01$, where the dependence on $\delta$ is leveled off, and such curves are displayed in Figs. 1 and 2 (for $R_0^3\delta = 10^{-3}$).

The common feature of Figs. 1 and 2 is the variation of $L_X$ over the whole possible region, from the minimum value of $L_X \approx R_0$ (an extremely strong localization) to the maximum of $L_X \sim R_c$ (the full delocalization). For small $|X|$, the eigenmodes are fully delocalized, $L_X \sim R_c$. As $|X|$ increases, $L_X$ start to decrease demonstrating the eigenmode localization. Comparing the data for $X>0$ and $X<0$, one concludes that the dispersion curves $L_X(X)$ are asymmetric with respect to the reversal $X \leftrightarrow -X$, which reflects the corresponding asymmetry of the exact eigenvalue problem. However, in the limit of $R_0^3|X| \gg 1$, the curves become symmetrical. This can be understood if one recalls that in the last case the binary approximation[3,7,9] becomes applicable, rendering the symmetric spectrum of eigenmodes [see Eq. (19) and its discussion].

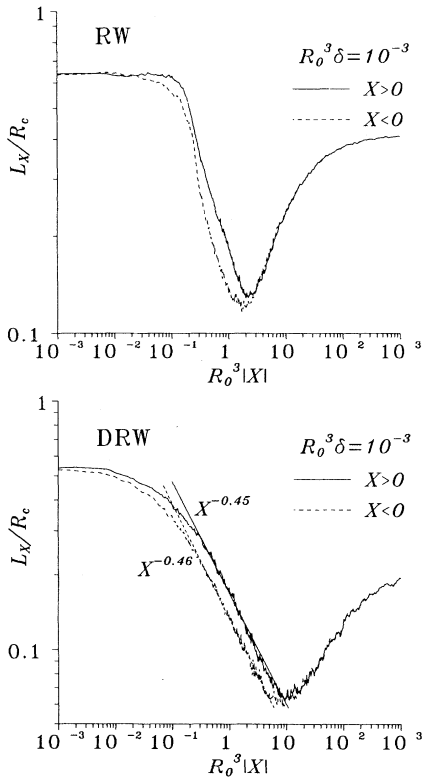


FIG. 1. Dispersion relation, i.e., normalized coherence length $L_X/L_c$ of eigenmodes as a function of the dimensionless spectral variable $R_0^3|X|$, for RW (upper panel) and DRW (lower panel) clusters. The curve for $X>0$ is shown by the solid line and for $X<0$ by a dashed line. For DRW, the best power fits and the corresponding indices are indicated. Note the double-logarithmic scale.

In the region $R_0^3|X| \gtrsim 1$, there are sharp dips present in the profiles, pronounced for CCA and DCCA clusters (Fig. 2). However, these fine structures for CCA and DCCA are not random and are fully reproducible for different Monte Carlo samples (data not shown). We will explicitly demonstrate this fact in Sec. IV for the polarizabilities. Each of these dips represents an eigenmode or close eigenmodes localized principally on pairs of monomers or groups of a few monomers. Because the CCA clusters are generated on a lattice, there exists only a small number of different configurations of the nearest neighbors, bringing about a few peaks and dips seen clearly in Fig. 2 (the upper panel) for $R_0^3|X| = 1-10$. The decimation is expected to decrease the amplitude and increase the number of these oscillations, eliminating them completely in the limit of indefinitely large dilution ($\beta \to 0$). However, $\beta$ cannot be made very small for the DCCA clusters due to the limitations of both the memory and the CPU time involved in the generation of the original CCA clusters. Realistically, in the calculations of the present scale, $\beta$ cannot be made considerably smaller than the achieved value of 0.07, otherwise the original clusters would have become too large. Consequently, the elements of the clusters' primary structure are not completely eliminated when generating the DCCA clusters. The amplitude of the peaks for $R_0^3|X| \sim 1-10$ (see Fig. 2) is significantly reduced for the DCCA clusters in comparison with CCA, and some peaks appear at much larger $X$, up to $R_0^3|X| \sim \beta^{-3/D}$, as expected.

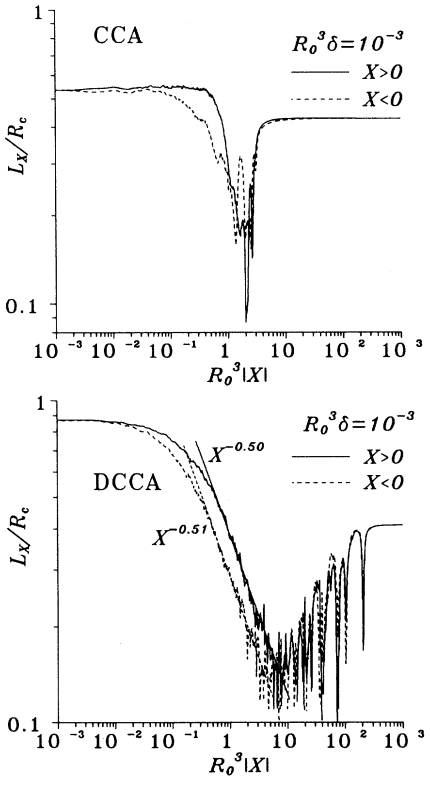


FIG. 2. The same as in Fig. 1 but for CCA (the upper panel) and DCCA (the lower panel).

In contrast to CCA and DCCA (Fig. 2) there is no significant manifestation of such localized eigenmodes for RW and DRW clusters (no pronounced peaks are seen in Fig. 1). This is due to the fact that the RW clusters are generated not on a lattice as CCA, but rather with continuous randomly chosen length and direction of elementary steps (see above in this section). Therefore all configurations of monomers at the minimum scale are different, and the corresponding peaks are randomly shifted and smoothed out. The same is true for DRW and, additionally, the high degree of the dilution ($\beta = 10^{-4}$) virtually eliminates any ordering at the minimum scale in this case.

In the extreme limit of very large $R_0^3|X|$, the localization length (Figs. 1 and 2) tends to some constant intermediate between $R_0$ and $R_c$. In this case, the spectral variable $X$ is out of the range of the eigenvalues $w_n$, and consequently all eigenmodes irrespectively to $w_n$ are excited with equal weights due to the tails of the Lorentzian contours, $\nu_n(X) \sim X^{-2}$. Note that in these tails the absorption of the cluster is very low, and such high values of $X$ may be physically unreachable for some clusters.

The maximum value of $L_X$ in Figs. 1 and 2 is less than $R_c$, which may attribute to the factor of shape. In fact, each of the random clusters is not spherically symmetric, but eigenmodes tend to be. Therefore, the eigenmodes are limited by the minimum size of a given cluster and cannot occupy the total volume of the cluster even when they are fully delocalized. To support this interpretation, we show in Fig. 3 the dispersion curves calculated for "random gas" (RG) clusters, i.e., for random clusters consisting of spatially uncorrelated monomers contained within a sphere of a given radius. In this case, all the clusters are spherically symmetric, and the maximum $L_X$ is very close to $R_c$. The region of the localization is narrower for RG than for the diluted fractals, otherwise their dispersion curves are similar. It is our expectation that asymptotically for $N \to \infty$ the slope for RG will become infinitely large for $X \lesssim 1$ exhibiting the dispersionless behavior of the plasmons, while for the fractals it will

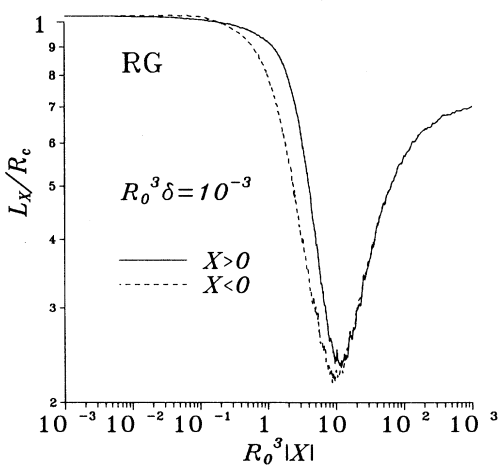


FIG. 3. Dispersion relation of eigenmodes for RG clusters for $X > 0$ (solid line) and $X < 0$ (dashed line).

approach a finite value [cp. Eq. (13)].

Comparing the diluted vs original (nondiluted) fractals (the lower and upper panels in Figs. 1 and 2) and the RG clusters (Fig. 3), we conclude that the transition from extremely localized to completely delocalized eigenmodes occurs in a much wider region for the diluted fractals. Correspondingly, the prospective scaling region of Eq. (10) is much narrower for the nondiluted fractals. For the CCA fractals, the transition region is so narrow that for the present $N$ there exists no hope of actually seeing any scaling.

The initial idea of the introduction of the diluted clusters in Ref. 7 is that the dilution simplifies the local structure but does not affect the correlations on the scale of $r \gg R_0$. Therefore, the hope was that in the intermediate region (10) dilution would not affect the eigenmodes, and therefore the dilutions would not change forms of the spectral dependencies, including scaling indices, as it does not change, in particular, the Hausdorff dimension $D$. Contrary to this assumption, the dramatic difference between the diluted and undiluted clusters seen in Figs. 1 and 2 poses a problem for the theory. There are possibly two different explanations of this fact. First, it is feasible that even for long-range excitations ($L_X \gg R_0$), small-scale ($r \sim R_0$) features of the eigenmodes are still important. This may be the case if the eigenmodes possess singularities at the small scale. The second possible interpretation is that the diluted clusters are actually representatives of their parent original clusters which are much larger ($N \propto \beta^{-1}$). This interpretation implies that for larger and larger undiluted clusters the difference caused by the dilution would be diminished and eventually erased. Both of these explanations are feasible on the basis of the available information.

A point of principal importance is scaling of the dispersion curves predicted in Ref. 7, as described by Eq. (15). From Figs. 1 and 2 (the upper panels) one can see that there actually exists no scaling for the undiluted fractals, as anticipated above. In contrast, the diluted fractals (see the lower panels) possess regions which can be interpreted as scaling, though even for the maximum $N = 300$ the widths of these regions in $X$ are only slightly more than a decade. Therefore, our conclusion is that for the diluted fractals the present data are compatible with the scaling. The scaling indices $\theta$ found from the data of Figs. 1 and 2, the values of $d_o$ calculated with the aid of Eq. (13), and the values of $D$ are summarized in Table I. Interestingly enough, the indices for $X > 0$ and $X < 0$ coincide within 0.01 (which we believe to be the statistical accuracy of the present data). This equality of the indices is not trivial because, as we have already indicated, there is no exact $X$-reversal symmetry.

TABLE I. Summary of the scaling indices $\theta$ found from the data of Figs. 1 and 2, the values of $d_o$ calculated with the aid of Eq. (13), and the values of $D$.

| | | $X>0$ | | $X<0$ | |
|---|---|---|---|---|---|
| Cluster type | $D$ | $\theta$ | $d_o$ | $\theta$ | $d_o$ |
| DRW | 2.00 | 0.45 | 0.55 | 0.46 | 0.54 |
| DCCA | 1.75 | 0.50 | 0.38 | 0.51 | 0.36 |

Another point of importance is the dependence of the surface-plasmon dispersion on cluster size. To investigate this, in Fig. 4 we compare the dispersion curves for the diluted clusters with $N = 300$ and $N = 100$. One can see that the slopes ($\theta = 0.37$ for DRW and $\theta = 0.41$ for DRW) are significantly smaller than those found for $N = 300$ (see Table I). Also, the regions of scaling for $N = 100$ are substantially narrower, as expected on the grounds of Eq. (14). Actually on the basis of the $N = 100$ data alone, it would have been impossible to distinguish the narrow scaling region from an inflation point.

The results published previously[18] for DCCA for a comparable size ($N = 128$) clusters have given the value (for $X > 0$) of $\theta = 0.52 \pm 0.07$ which significantly differs from the present value of $\theta = 0.41$. The reason for this difference lies in much higher statistical noises evident in the data of Ref. 18. Actually, on the basis of the data of Ref. 18 it is impossible to conclude on the shape of the dispersion curve, in particular, on the existence of the scaling (we will return to the discussion of this point below in Sec. IV).

Because the effective scaling index $\theta$ changes (increases) with $N$ (and the corresponding $d_0$ decreases), it is legitimate to consider two questions: (i) whether the limiting (for $N \to \infty$) slope is finite, and if so (ii) whether the present size of the clusters ($N = 300$) is sufficient to find the true value of $\theta$ ($N = 100$ is certainly insufficient). As

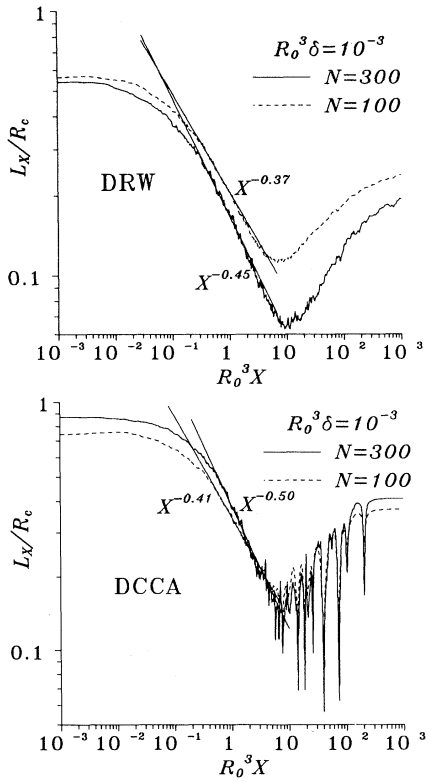


FIG. 4. Dispersion relations for DRW (upper panel) and DCCA (lower panel) for $N = 300$ (solid line) and $N = 100$ (dashed line). The best-fit lines and the corresponding indices are indicated.

we have mentioned above in the conjunction with the RG clusters, our expectation is that $\lim_{N\to\infty}\theta$ is finite for fractals and infinite for three-dimensional systems such as the RG clusters. However, to answer these questions with certainty, one must invoke much larger clusters (at least with $N\sim 10^3$). However, this is unrealistic to do employing the present method (though it appears to be the most efficient of the known methods), because the present project has consumed over 120 h of CPU time on the Cray Y-MP/C90 computer (at the Pittsburgh Supercomputer Center), even with the maximum extent of the vectorization.

## IV. NUMERICAL RESULTS: LINEAR POLARIZABILITY

We will concentrate on the imaginary part of the polarizability, Im$\alpha$, which is of special importance because the absorption of a cluster per monomer is proportional to Im$\alpha$. We will occasionally refer to this quantity simply as absorption. The results of the calculation of Im$\alpha(X)$ for RW and DRW ($\beta=10^{-4}$) clusters are shown in Fig. 5 (the upper and lower panels, respectively). Similar results for CCA and DCCA ($\beta=0.07$) are shown in Fig. 6. As in the case of dispersion curves (Sec. III), we express all results in terms of the scaled variables $R_0^3|X|$, $R_0^3\delta$, and $R_0^{-3}\mathrm{Im}\alpha$. Owing to such a choice, the results do not depend on the total spatial scale of the clusters [cp. Eq. (9)].

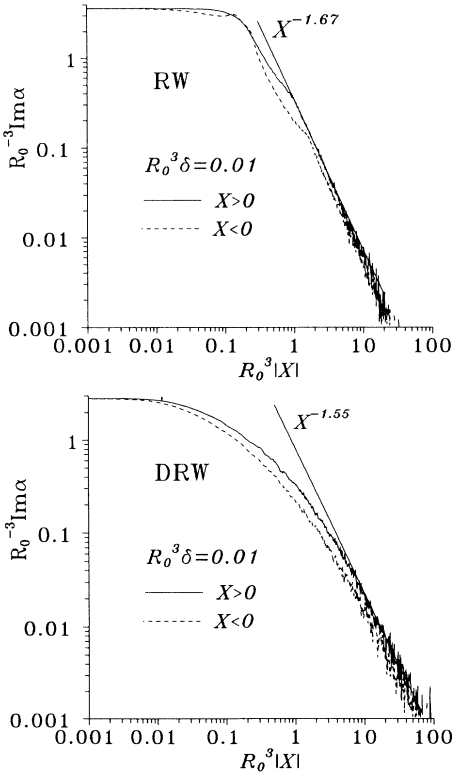


FIG. 5. Normalized absorption contour, i.e., $R_0^{-3}\mathrm{Im}\alpha$ as a function of $R_0^3|X|$ for RW (upper panel) and DRW (lower panel). The data are shown for $X>0$ (solid line) and $X<0$ (dashed line) for $R_0^3\delta=0.01$. The best-fit lines for $R_0^3|X|\gg 1$ and the corresponding indices are indicated.

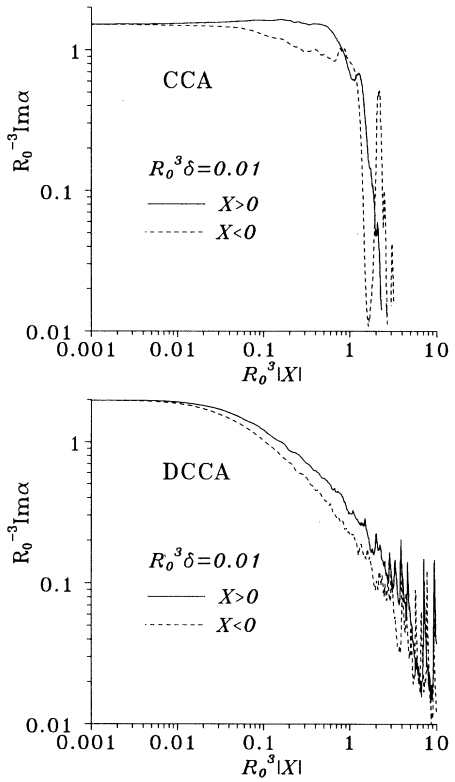


FIG. 6. The same as in Fig. 5 but for CCA (upper panel) and DCCA (lower panel) clusters.

The absorption profiles are calculated for the dissipation parameter $R_0^3\delta=10^{-2}$, which is realistic for coinage-metal clusters in the visible range.

For all four types of clusters shown in Figs. 5 and 6, the absorption profiles are broad contours, asymmetric in $X$, in agreement with the asymmetry of the eigenvalue problem with respect to the $X$ reversal. There are no individual spectral lines resolved for $R_0^3|X|\lesssim 1$. For $R_0^3|X|\gtrsim 1$, individual peaks are resolved for CCA and DCCA clusters (Fig. 6), and noiselike dense structures of much smaller amplitude are seen for RW and DRW clusters (Fig. 5). Similar to the dispersion curves (Sec. III), the peaks for CCA and DCCA clusters are fully reproducible for different Monte Carlo samples (see below in this section) and represent excitations localized on only a few monomers. As in Sec. III, the number of these peaks is larger but their amplitude is smaller for the diluted than for the original fractals. We expect that for indefinitely large dilutions ($\beta\to 0$), these structures in the spectra of diluted fractals will be completely eliminated.

In contrast to CCA and DCCA (Fig. 6), for RW and DRW clusters (Fig. 5), the noiselike structures have relatively small amplitudes and are not reproducible between different clusters. Thus, these structures are likely to be due to statistical fluctuations caused by a finite, though large, size of the Monte Carlo sample. Similar to what is discussed above in Sec. III in the conjunction with Fig. 1, the absence of the well-defined and reproducible peaks for RW is due to the fact that for the RW clusters, which

are generated by a continuous random walk, there are no multiply repeating regular structures at the small scale, in contrast to CCA generated on a cubic lattice. An additional factor suppressing the peaks for DRW is the very high degree of dilution ($\beta=10^{-4}$) comparing to that of DCCA ($\beta=0.07$).

Smooth structureless contours obtained in the present calculations for $R_0^3|X| \lesssim 1$ are qualitatively in agreement with numerous experimental observations (see, e.g., Ref. 15). Quite different types of spectra consisting of a multifractal set of spectral lines and gaps were obtained for recursively built exactly self-similar fractals in Ref. 10. The difference between the present results and those of Ref. 10 lies in the random structure of clusters in the present paper and ordered deterministic structure in Ref. 10. When a cluster is random, the spectral lines for different realizations are randomly shifted, forming a smooth contour. In contrast, for the deterministic structures,[10] the spectral lines are strongly degenerate, their numbers are much smaller and, consequently, they are resolved in spectra.

Similar to what we have described for the dispersion curves (Sec. III), there is a striking difference between the diluted and undiluted clusters. The difference signifies that the small-scale behavior of the eigenmodes is important, which may be due to singularities of the eigenmodes at small distances and/or to the original clusters being not sufficiently large.

Especially important is the question of the scaling behavior of $\mathrm{Im}\alpha(X)$ [see Eq. (11)]. In Fig. 5, one can see pronounced scaling behavior extended over a decade in $X$ and almost two decades in $\mathrm{Im}\alpha(X)$ for RW and over shorter intervals for DRW. The scaling indices for $X>0$ and $X<0$ are practically coinciding despite the asymmetry of the eigenvalue problem. However, this is certainly not the kind of scaling described by Eq. (11), because the corresponding indices are greater than 1 in magnitude, while $d_o-1$ given by Eq. (11) should be less. Also, this scaling exists for $R_0^3|X| \gg 1$, contrary to the condition of Eq. (14).

The scaling for $R_0^3|X| \gg 1$ is that predicted by the binary approximation [Eq. (18)] whose index for RW and DRW is $-1.67$, in perfect agreement with the index ($-1.67$) for RW (the upper panel in Fig. 5) and in somewhat less agreement with the value of $-1.55$ for DRW (the lower panel). For DRW such scaling is expected (see the end of Sec. II), and we can safely associate it with the binary nature of the eigenmodes for $R_0^3|X| \gg 1$. For RW such a perfect "binarylike" scaling is to some extent puzzling. We can speculate the role of monomers for the binary approximation is played by larger collections of the monomers. In other words, the renormalization leads to a diluted-type cluster, bringing about this type of the scaling behavior.

As one can see for DCAA (Fig. 6, the lower panel), the scaling in the region $R_0^3|X| \gg 1$ is masked by the fine-structure peaks. This is evidence that the dilution parameter $\beta=0.07$ is not small enough to bring about the behavior of Eq. (18). In contrast to RW, no scaling behavior is observed for CCA (the upper panel in Fig. 6) for $R_0^3|X| \gg 1$.

Due to reasons described in Ref. 7, we do not expect the binary approximation to be applicable for RG clusters. In fact, the absorption profile for the RG clusters shown in Fig. 7 does have a region of scaling for $R_0^3|X| \gg 1$, but the index ($-1.9$) is very close to the one for free monomers ($-2.0$). In other words, the broadening of the absorption spectrum by the randomness of the clusters is not strong enough, and the spectrum of individual monomers $\mathrm{Im}\alpha=\delta/(X^2+\delta^2)$ transpires for $R_0^3|X| \gg 1$ as $\mathrm{Im}\alpha \propto X^{-2}$. Otherwise, the absorption profile for RG clusters is similar to those for the diluted clusters.

The most puzzling feature of the absorption spectra shown in Figs. 5 and 6 is an absence of any pronounced scaling behavior in the collective region (14), even for the diluted clusters. This finding contradicts the earlier observations of such a scaling in Refs. 7, 9, and 17. The scaling observed in these references is spurious and is due to large fluctuations of the data because of insufficient Monte Carlo statistics. The absence of the scaling in the collection region is all the more puzzling given that the dispersion curves for the diluted clusters do possess regions of scaling (see Sec. III, Figs. 1 and 2).

To rationalize the absence of the scaling of $\mathrm{Im}\alpha$ in the collective region, we can attribute it basically to the same two reasons as we have already mentioned above in connection with the effect of the dilution on the dispersion curves (Sec. III) and the absorption profiles: (i) the clusters are not large enough, and the excitations which are much smaller than $R_c$ become comparable with $R_0$; and/or (ii) the eigenmodes are singular at the minimum scale. We note that the dependence of index $\theta$ on $N$ observed for the dispersion curves (see Fig. 4 and the corresponding discussion in Sec. III) suggests that the first reason (i) may contribute.

To distinguish between these two reasons, we consider explicitly the dependence of the absorption on cluster size. In Fig. 8 we present the comparison of the absorption spectra of CCA and DCCA for $N=100$ and $N=300$ The results of this test are quite different from those for the dispersion curves (Fig. 4). Namely, we see from Fig. 8 that the threefold increase of $N$ from 100 to 300 does

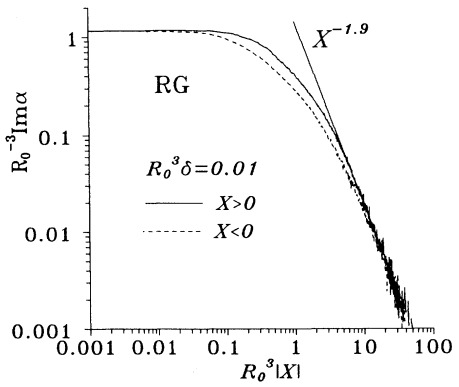


FIG. 7. Normalized absorption contour for RG clusters for $X>0$ (solid line) and $X<0$ (dashed line).

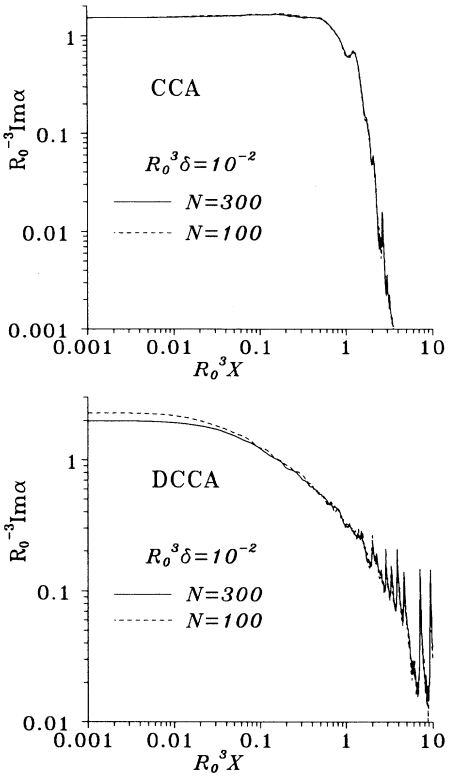


FIG. 8. Comparison of the absorption contours for $N=300$ (solid line) and $N=100$ (dashed line). The data are shown for CCA (upper panel) and DCCA (lower panel).

not have any noticeable effect on CCA and has only a minor effect on DCCA. Exactly the same conclusions can be drawn from similar data on RW and DRW (graphs not shown). These results imply that the interactions at the maximum scale do not contribute significantly to the absorption (but they do to the localization radius). Thus, we conclude that the absorption is mostly determined by the interaction at the small to intermediate scale ($r \ll R_c$). Additional support to this result is given by the fact that the resolved peaks in Fig. 8 at $R_0^3 X \gtrsim 1$ are virtually the same for $N=100$ and $N=300$, in agreement with our previous conclusion that these peaks originate from extremely localized eigenmodes.

As a side product of this test, we notice that the peaks of the absorption for $N=100$ and $N=300$ in Fig. 8 exactly coincide. Because the data for the two values of $N$ are statistically independent, this implies that these peaks are not random, in agreement with their interpretation as stemming from eigenmodes localized on small elements of the cluster structure (in particular, the pairs of monomers). Finally, we note that the above-presented test is indeed not a proof. It is feasible in principle that for much larger $N$ the absorption spectra would change and scale with $X$. As we have already indicated at the end of Sec. III, it is unlikely that the case of much larger $N$ will be technically possible to explore numerically in the near future.

For the sake of brevity, we do not show the data for the eigenmode densities [Eq. (6)]. The spectral dependences $\nu(X)$ are in fact very close to the absorption profiles $\mathrm{Im}\alpha(X)$. The result of Ref. 7 that $\pi\nu(X)\approx 3\,\mathrm{Im}\alpha(X)$ is confirmed by the present data with much higher statistical accuracy. We note that this result means that all eigenmodes on the average contribute with equal weight to the absorption.[7,9]

To obtain more insight into the unexpected behavior of the absorption, we would like to suggest a new plot, namely $\mathrm{Im}\alpha$ as a function of the coherence length $L_X$. This plot has a fundamental advantage of both the function and its argument being potentially scale invariant. In contrast, $X$ is not scale invariant and changes with the minimum scale as[9] $X \propto R_0^{-(3d_o-D)/(d_o-1)}$. Another advantage of this plot is that the expected scaling index depends only on the Hausdorff dimension $D$, $\mathrm{Im}\alpha \propto L_X^{3-D}$ [see Eq. (12)]. It is important that underlying Eq. (12) is based only on very general assumptions, namely Eq. (10) and strong localization and is independent on the way the variable $X$ behaves under the scale renormalization.

The plot $\mathrm{Im}\alpha(L_X)$ is presented in Fig. 9 for RW and DRW (upper panel) and for CCA and DCCA (lower panel). As one can trace in the figure, the function $\mathrm{Im}\alpha(L_X)$ consists of two branches. The lower branch corresponds to $R_0^3|X| \gg 1$ and no scaling behavior is expected for it. In contrast, the upper branch corresponds to the intermediate region of Eq. (10) and the scaling for

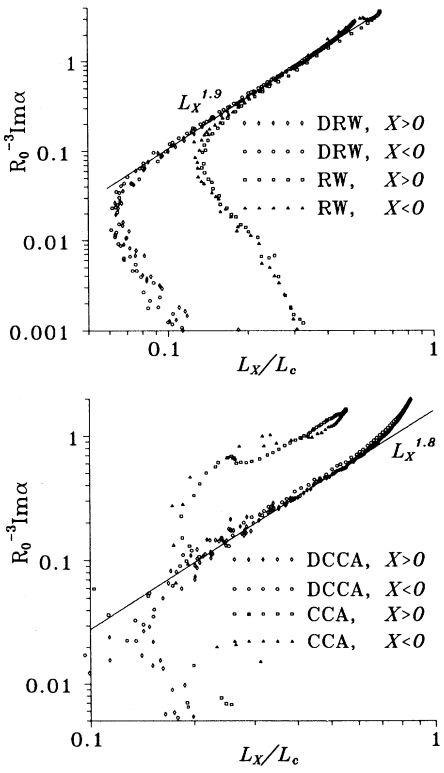


FIG. 9. The dispersion relations for RW and DRW (upper panel) and CCA and DCCA (lower panel) as functions of the normalized coherence length. Notations are shown in the figure, where the best-fit lines and indices are indicated.

it is predicted by Eq. (12). For RW and DRW, the upper branch does possess a developed scaling behavior, extended for DRW over most of the variation of the absorption (about one decade in Im$\alpha$). Interestingly enough, RW and DRW exhibit almost the same scaling, while on the plots Im$\alpha(X)$ (cp. Fig. 5) and $L_X(X)$ (cp. Fig. 1) their behavior is substantially different. The same is true also for the dependences for $X>0$ and $X<0$ which completely collapse into one curve. These facts would have been in agreement with the universal scaling of Eq. (12), but the value of the index found (1.9) differs dramatically from 1.0 predicted by Eq. (12).

The picture for CCA and DCCA (lower panel in Fig. 9) is somewhat less definite though generally similar to that described just above. The curves for $X>0$ and $X<0$ do collapse onto a common line, but those for CCA and DCCA are different, though one can see a certain trend for them to be parallel. Again, the scaling index found for DCCA (1.8) substantially exceeds the expected value of 1.25.

The findings presented in the two paragraphs above indicate again that the absorption is not completely scale invariant. Whether this is due to the clusters not being large enough or is an intrinsic property of the eigenmodes (singularity at the minimum scale?) still remains an open question.

## V. CONCLUDING DISCUSSION

This paper fills an essential gap in the previous knowledge of the linear optical (dipolar) responses of fractals. It provides accurate high-resolution data for the dispersion curves $L_X$ and the linear absorption spectra Im$\alpha$ for different fractals (RW, DRW, CCA, and DCAA) and fractally trivial random-gas (RG) clusters. Both the CPU time (more than 120 h on the Cray Y-MP/C90 at the Pittsburgh Supercomputer Center plus 800 h on the IBM 3090 at Washington State University) and memory requirements (up to 8 megabytes) and disk space (35 gigabytes) are characteristic of a large-scale computational project.

Some of the findings obtained from these data are quite unexpected, contradicting the previous much less accurate numerical studies. Most of the discussion of the results obtained is incorporated into the text of Secs. III and IV. In this concluding section, we intend to summarize only the principal findings of the present paper.

(i) the scaling of the dispersion relation $L_X(X)$ predicted in Ref. 7 [see Eq. (13)] takes place for the diluted fractals (DRW and DCCA) [see Figs. 1 and 2 (lower panels)]. However, such scaling is absent for the original clusters (RW and CCA, see the upper panels in the same figures) which we can attribute to an insufficient size of these clusters (in contrast, the diluted clusters are representatives of their much larger parent clusters). The region of scaling for DRW and DCCA is intermediate, in agreement with the scaling condition of Eq. (10). In this region, the elementary excitations (eigenmodes or surface plasmons) are collective, i.e., delocalized over many monomers, but still well localized within a cluster. The scaling indices are practically equal for negative and positive $X$, despite the asymmetry of the problem in general. There exists a considerable dependence of the dispersion curves on the cluster size from $N=100$ to 300 (see Fig. 4). Whether this dependence is fully saturated for $N\geq 300$ remains a question.

(ii) There is no evident scaling of the absorption spectra Im$\alpha(X)$ in the intermediate region (14) for any of the clusters studied (see Figs. 5 and 6). The absorption spectra are essentially independent on the cluster size for $N=100$ to 300 (Fig. 8). These findings suggest that the interaction at the minimum scale ($r\sim R_0$) may be responsible for the absence of scaling. In turn, such interaction may be important due to two possible reasons, namely, insufficient size of clusters, or singularity of the eigenmodes at the small scale. The independence of the absorption (per monomer) of $N$ suggests that the minimum-scale singularity is a likely reason.

(iii) A new plot suggested in this paper, Im$\alpha(L_X)$ (see Fig. 9), does reveal scaling of the absorption as a function of the coherence length in the intermediate region (14) (such scaling for CCA is less pronounced due to interference of strongly localized eigenmodes, caused by insufficient size of the clusters). The scaling indices are equal for $X>0$ and $X<0$ despite the asymmetry of the problem with respect to the $X$ reversal. However, these indices (1.9 for RW and DRW and 1.8 for DCCA) differ significantly from the predictions of the strong-localization scaling theory [Eq. (12) yields the values of the indices of 1.0 and 1.25, respectively]. This finding again demonstrates that there exists no full-scale invariance for the present clusters.

(iv) Finally, we have observed for DRW (see Fig. 5) a scaling with the index close to $1+D/3$ predicted by the binary approximation[7] (18) for diluted clusters in the spectral wings, $R_0^3|X|\gg 1$. Surprisingly, a scaling with the predicted index is also found for nondiluted clusters, namely, RW. Similar scaling for DCCA is masked by the fine-structure peaks present due to an insufficient decimation for such clusters (achieving a larger decimation is difficult due to the CPU-time limitations).

Of all the results mentioned above, the most puzzling is the absence of any conspicuous intermediate-region scaling (11) for the absorption Im$\alpha(X)$ in the presence of such scaling for the dispersion relation $L_X(X)$. An insufficient size of the clusters is not very likely to be a single reason for this, because there is virtually no change in the absorption for $N=100$ to 300. A more likely reason is a considerable contribution to the absorption originating at the minimum spatial scale. Such a contribution may be important for the absorption despite a large coherence length of the excitations due to possible singularity of eigenmodes at the minimum scale. At the same time, the coherence length, by its definition, neglects extremely localized states, thus allowing scaling. However, this is a conjecture, and obtaining the final answer to this puzzle is still ahead.

## ACKNOWLEDGMENTS

This research was supported by the NSF under Grant No. CHE-9196214 and by the Pittsburgh Supercomputing Center under Grant no. PHY890020P. We are grateful to Ronald Fuchs for useful discussions.

*Also with the Institute of Automation and Electrometry, Russian Academy of Sciences, Novosibirsk 630090, Russia.
†Present address: Department of Physics, West Virginia University, Morgantown, West Virginia 26506.

[1]M. V. Berry and I. C. Percival, Opt. Acta **33**, 577 (1986).
[2]P. M. Hui and D. Stroud, Phys. Rev. B **33**, 2163 (1986).
[3]V. M. Shalaev and M. I. Stockman, Zh. Eksp. Teor. Fiz. **92**, 509 (1987) [Sov. Phys. JETP **65**, 287 (1987)].
[4]A. V. Butenko, V. M. Shalaev, and M. I. Stockman, Zh. Eksp. Teor. Fiz. **94**, 107 (1988) [Sov. Phys. JETP **67**, 60 (1988)].
[5]S. G. Rautian, V. P. Safonov, P. A. Chubakov, V. M. Shalaev, and M. I. Stockman, Pis'ma Zh. Eksp. Teor. Fiz. **47**, 200 (1988) [JETP Lett. **47**, 243 (1988)].
[6]A. V. Karpov, A. K. Popov, S. G. Rautian, V. P. Safonov, V. V. Slabko, V. M. Shalaev, and M. I. Stockman, Pis'ma Zh. Eksp. Teor. Fiz. **48**, 528 (1988) [JETP Lett. **48**, 571 (1988)].
[7]V. A. Markel, L. S. Muratov, and M. I. Stockman, Zh. Eksp. Teor. Fiz. **98**, 819 (1990) [Sov. Phys. JETP **71**, 455 (1990)].
[8]A. V. Butenko, P. A. Chubakov, Yu. E. Danilova, S. V. Karpov, A. K. Popov, S. G. Rautian, V. P. Safonov, V. V. Slabko, V. M. Shalaev, and M. I. Stockman, Z. Phys. D **17**, 283 (1990).
[9]V. A. Markel, L. S. Muratov, M. I. Stockman, and T. F. George, Phys. Rev. B **43**, 8183 (1991).
[10]F. Claro and R. Fuchs, Phys. Rev. B **44**, 4109 (1991).
[11]M. I. Stockman, T. F. George, and V. M. Shalaev, Phys. Rev. B **44**, 115 (1991).
[12]M. G. Kuzyk, M. P. Andrews, U. C. Paek, and C. W. Dirk, SPIE Proc. **1560**, 44 (1991).
[13]M. I. Stockman, T. F. George, and V. M. Shalaev, Phys. Rev. B **44**, 115 (1991).
[14]V. M. Shalaev, M. I. Stockman, and R. Botet, Physica A **185**, 181 (1992).
[15]Yu. E. Danilova, A. I. Plekhanov, and V. P. Safonov, Physica A **185**, 61 (1992).
[16]M. I. Stockman, V. M. Shalaev, M. Moskovits, R. Botet, and T. F. George, Phys. Rev. B **46**, 2821 (1992).
[17]V. M. Shalaev, R. Botet, and R. Julien, Phys. Rev. B **44**, 12 216 (1992).
[18]V. M. Shalaev, R. Botet, and A. V. Butenko, Phys. Rev. B **48**, 6662 (1993).
[19]M. G. Kuzyk, M. P. Andrews, and F. Ghebremichael, Nonlinear Opt. **6**, 103 (1993).
[20]X. Zhang and D. Stroud, Phys. Rev. B **49**, 944 (1994).
[21]M. I. Stockman, L. N. Pandey, L. S. Muratov, and T. F. George, Phys. Rev. Lett. **72**, 2486 (1994).
[22]D. P. Tsai, J. Kovacs, Z. Wang, M. Moskovits, V. M. Shalaev, J. S. Suh, and R. Botet, Phys. Rev. Lett. **72**, 4149 (1994).
[23]F. Brouers, D. Rauw, J. P. Clerc, and G. Giraud, Phys. Rev. B **49**, 14 582 (1994).
[24]Eigenmodes contributing to optical polarizabilities are dipolar. It is conventional to call electronic dipolar excitations as plasmons. For systems much smaller in size than the light wavelength $\lambda$, such eigenmodes are traditionally called surface plasmons, though they may actually occupy the whole volume of a system. We will adhere to such a terminology in our consideration of fractal clusters, though it wold be logical to call their eigenmodes as "cluster plasmons" rather than surface plasmons. The frequencies of surface plasmons of a system can approximately be found from the equation $\mathrm{Re}\alpha=0$, where $\alpha$ is its polarizability. Note that for a system much larger in size than $\lambda$, the corresponding dipolar excitations would be polaritons.
[25]T. C. Halsey, M. H. Jensen, L. P. Kadanoff, I. Procaccia, and B. I. Shraiman, Phys. Rev. A **33**, 1141 (1986).
[26]J. E. Sipe and R. W. Boyd, Phys. Rev. B **46**, 1614 (1992).
[27]In this paper we denote the polarizability conventionally as $\alpha$ rather than $\chi$ as in our previous publications. This notation should not be confused with the index $\alpha$ in subscripts denoting a vector coordinate.
[28]R. Fuchs and F. Claro, Phys. Rev. B **39**, 3875 (1989).
[29]J. K. Cullum, *Lanczos Algorithms for Large Symmetric Eigenvalue Computations* (Birkhausen, Boston, 1985).
[30]P. Meakin, Phys. Rev. Lett. **51**, 1119 (1983).
[31]M. Kolb, R. Botet, and R. Jullien, Phys. Rev. Lett. **51**, 1123 (1983).